RSC Advances

Graphical Abstract

COX-1

COX-2

CA-DE

Among the 9 synthesized derivatives of hydroxycinnamic acids, diethyl esters selectively inhibited COX-2 enzyme. The most active compound was caffeic acid diethyl ester (CA-DE) with 88.5/30.5% inhibition at 100/20 µM against COX-2, while its COX-1 inhibition was negligible. Docking studies showed that CA-DE forms 3 hydrogen bonds with the active site of COX-2, while it forms only the first two bonds with COX-1.

RSC Advances

ARTICLE

Hydroxycinnamic acid as a novel scaffold for the development of cyclooxygenase-2 inhibitors

T. Silva,[a] F. Borges,[a†] N. Edraki,[b] M. Alizadeh,[b] R. Miri,[b] L. Saso[c] and O. Firuzi[b†]

Cyclooxygenase (COX) enzymes are involved in inflammation and cancer. Nine derivatives of hydroxycinnamic acids including ethyl and diethyl esters were synthesized and tested as COX inhibitors in whole blood assay. Esterification improved COX-1 and COX-2 inhibitory activities of the derivatives. Ethyl esters were more effective against COX-1 and the most potent one was caffeic acid ethyl ester. Interestingly, diethyl esters showed selectivity towards COX-2; The most active compound was caffeic acid diethyl ester (CA-DE) with 88.5 and 30.5% inhibitions against COX-2 at 100 and 20 μM, respectively, while it was almost inactive against COX-1. Docking studies showed that CA-DE forms 3 hydrogen bonds with the active site of COX-2 (4-OH..OH-Tyr355, 4-OH..NH-Arg120 and C=O..OH-Tyr385), while it forms only the first two bonds with COX-1. Furthermore, Val523 residue in COX-2 provides a wide hydrophobic pocket, which would accommodate diethyl esters. The present approach inspired by a natural scaffold provides an asset for the generation of new chemical entities endowed with selective COX-2 inhibitory activity.

1 Introduction

Cyclooxygenase (COX or PGH synthase) is a membrane-bound heme protein and the key rate-limiting enzyme involved in the arachidonic acid metabolism and prostanoid biosynthesis.[1] This enzyme exists at least as two main isoforms (COX-1 and COX-2), which have a high degree of homology, but possess different tissue distributions and physiological functions.[2] COX-1, the house-keeping isoform, is constitutively expressed in many tissues and mediates cytoprotective function in the gastric mucosa and tissue homeostasis through the production of prostaglandins (PGs). The inducible enzyme, COX-2, is overexpressed in response to a variety of mitogenic or pro-inflammatory stimuli and is mainly involved in the production of different PGs in the inflamed as well as neoplastic tissues.[3, 4] The pathological role of COX-2 in progression of cancer and different inflammatory processes has made this enzyme a valuable pharmacological target for drug discovery programs, namely those related with inflammation. Furthermore, application of COX-2 inhibitors for prevention or treatment of cancer has been recently suggested by several groups.[5]

[a] CIQ/Department of Chemistry and Biochemistry, Faculty of Sciences, University of Porto, 4169-007 Porto, Portugal
[b] Medicinal and Natural Products Chemistry Research Center, Shiraz University of Medical Sciences, Shiraz, Iran
[c] Department of Physiology and Pharmacology "Vittorio Erspamer", Sapienza University of Rome, Rome, Italy
† Addresses for correspondence:
Omidreza Firuzi, MD, PhD. Medicinal and Natural Products Chemistry Research Center, Shiraz University of Medical Sciences, Shiraz, Iran. Tel: +98-711-230-3872, Fax: +98-711-233-2225. Email: firuzio@sums.ac.ir
Fernanda Borges, PhD. CIQ/Department of Chemistry and Biochemistry, Faculty of Sciences, University of Porto, 4169-007 Porto, Portugal. Email: fborges@fc.up.pt

Highly prescribed non-steroidal antiinflammatory drugs (NSAIDs) such as ibuprofen and indomethacin are a heterogeneous group of compounds containing for instance ester or carboxylic groups (Fig. 1). NSAIDs act through the inhibition of COX-1 and COX-2 and are widely used for the treatment of a vast range of diseases ranging from chronic inflammatory conditions such as rheumatic diseases to fever and pain [6] and may also be protective against Alzheimer's disease [7] and cancer.[5,8] However, various gastrointestinal adverse effects such as ulceration and even GI bleeding are common side effects associated with the long term use of nonselective classical NSAIDs.[9] These side effects are mainly attributed to COX-1 inhibition and the absence of selectivity towards COX-2.[10] Due to these caveats, the identification of new chemical entities with improved safety profiles and preferably increased selectivity towards COX-2 isoform is still a hot topic. Drugs containing diaryl moieties attached to a central heterocyclic ring scaffold (tricyclic derivatives, i.e. celecoxib and rofecoxib) or on the adjacent sp^2 hybridized carbons of acyclic template (non-tricyclic template) (Fig. 1) have been introduced as selective COX-2 inhibitors. The structure-activity relationship (SAR) of diarylheterocycles as selective COX-2 inhibitors has been extensively investigated.[1,11] However, serious concern has been raised about the adverse cardiovascular effects of this type of drugs [12,13] and safer drug candidates are still needed, namely the development of drugs with a moderate selectivity towards COX-2. Several lines of evidence have shown that the derivatization of the carboxylate moiety in substrate analogue inhibitors (e.g. indomethacin) yield potent and selective COX-2 inhibitors. For instance, the simple conversion of the free carboxylic acid of indomethacin to the corresponding methyl

ester afforded a potent and selective COX-2 inhibitor (IC_{50} COX-2 ~ 250 nM *vs* IC_{50} COX-1 ~ 33000 nM), and chain length extension to higher alkyl homologues unveiled significant increments in potency and selectivity for COX-2.[14]
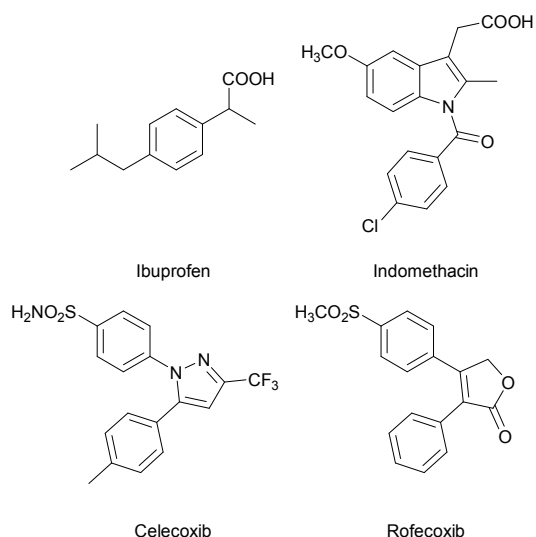

Figure 1. Chemical structures of cyclooxygenase inhibitors: classical non-steroidal antiinflammatory drugs (NSAIDs) (ibuprofen and indomethacin) andcoxibs (celecoxib and rofecoxib).

Furthermore, the development of NSAIDs based ester and amide derivatives has been extensively reported as a valid strategy to obtain analgesic and anti-inflammatory agents with no ulcerogenic activity, due to the considerable loss of COX-1 activity.[14-18] In fact, indomethacin esters such as indomethacin heptyl ester (Fig. 2A) have demonstrated enhanced selectivity towards COX-2.[14,18] Moreover, stilbene-like derivatives containing an acyclic central system including α,β-unsaturated core (*e.g.* resveratrol and derivatives thereof, Fig. 2) instead of the heterocyclic core of coxibs have been developed as novel selective COX-2 inhibitors.[11,19] Cinnamic acid (Fig. 2A) is currently considered a valid structure for drug discovery programs. In this regard hydroxycinnamic acids (HCAs) like coumaric and caffeic acid (Fig. 2A) are important naturally occurring phenolic compounds exhibiting a wide range of different biological activities, including anticarcinogenic, antioxidant and anti-inflammatory properties.[20-23] The modulation of the carboxylic acid function of naturally occurring HCAs, in accordance with the structural changes performed in commercially available NSAIDs, lead to ester type compounds (*e.g.* ethyl caffeate, Fig. 2A) able to suppress NF-κB and its downstream inflammatory mediators (iNOS, COX-2 and PGE2) in cellular models of inflammation.[24] Furthermore, several studies have shown the COX-2 inhibitory potential of HCA derivatives, including caffeic acid phenethyl ester (CAPE, Fig. 2A) isolated from ethanolic extract of propolis and also several ferulic acid derivatives.[19,25-29]
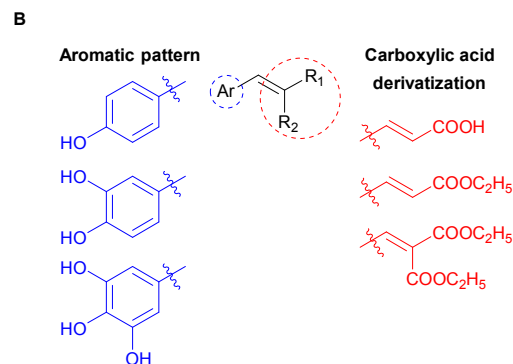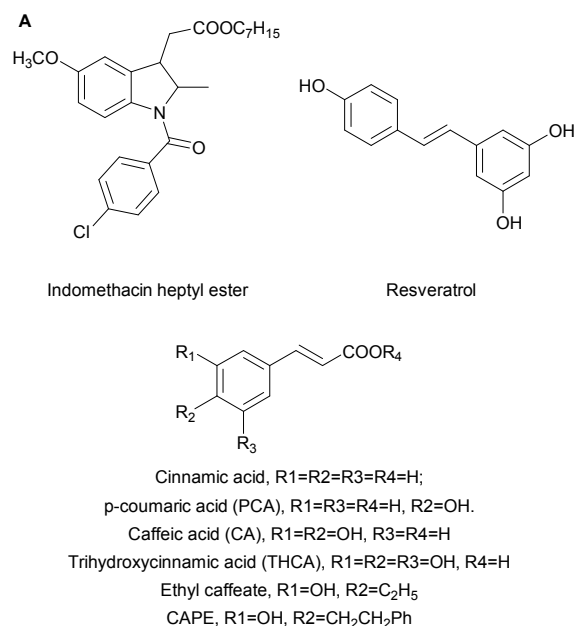

Figure 2A. Chemical structures of indomethacin heptyl ester and naturally-occurring COX-2 inhibitors; **2B** General structure of the HCA derivatives developed in this report.

In this context, the phenylpropanoid framework of HCAs can be further explored as scaffold for the development of selective COX-2, by derivatization of the carboxylic acid function (Fig. 2B). Furthermore, due to the structural similarities between resveratrol and HCAs, both sharing the hydroxyphenylethylene moiety, the rationale for the activity of HCAs on COX-2 is strengthened, providing a solid background for the development of COX inhibitors based on the HCA scaffold. In continuation of our previous studies on biological evaluation of various synthetic derivatives as COX inhibitors [30-33] we report the COX inhibitory activity of HCA derivatives (Fig. 2B) based on p-coumaric acid (PCA), caffeic acid (CA) and 3,4,5-trihydroxycinnamic acid (THCA). In addition, molecular docking studies were also conducted to identify the structural features required for the drug-enzyme (COX-2) interactions.

2 Results and discussion

2.1 Chemistry

Phenolic derivatives were obtained according to the synthetic strategies depicted in Scheme 1. Phenolic acids (commercially available or synthesized) and hydroxybenzaldehydes were converted to ethyl ester and diethyl esters. Generally, ethyl esters including p-coumaric acid ethyl ester (PCA-E), caffeic acid ethyl ester (CA-E) and 3,4,5-trihydroxy cinnamic acid ethyl ester (THCA-E) were obtained from the corresponding cinnamic acids by a microwave-assisted Fischer esterification. 3,4,5-Trihydroxy cinnamic acid (THCA) was obtained from 3,4,5-trihydroxybenzaldehyde following a Knoevenagel-Doebner condensation. The diethyl ester derivatives including p-coumaric acid diethyl ester (PCA-DE), caffeic acid diethyl ester (CA-DE) and 3,4,5-trihydroxy cinnamic acid diethyl ester (THCA-DE) were synthesized using the same chemical strategy. Overall, these reactions led to moderate yields of the desired compounds, which were then identified by nuclear magnetic resonance spectroscopy (^{1}H, ^{13}C NMR and DEPT) and electronic impact mass spectrometry (EI-MS). The spectroscopic results obtained for the synthesized compounds are in accordance with the data described in the literature.[34-36]

(THCA)

(PCA) R1=R3=H, R2=OH
(CA) R1=R2=OH, R3=H
(THCA) R1=R2=R3=OH

(PCA-E) R1=R3=H, R2=OH
(CA-E) R1=R2=OH, R3=H
(THCA-E) R1=R2=R3=OH

(PCA-DE) R1=R3=H, R2=OH
(CA-DE) R1=R2=OH, R3=H
(THCA-DE) R1=R2=R3=OH
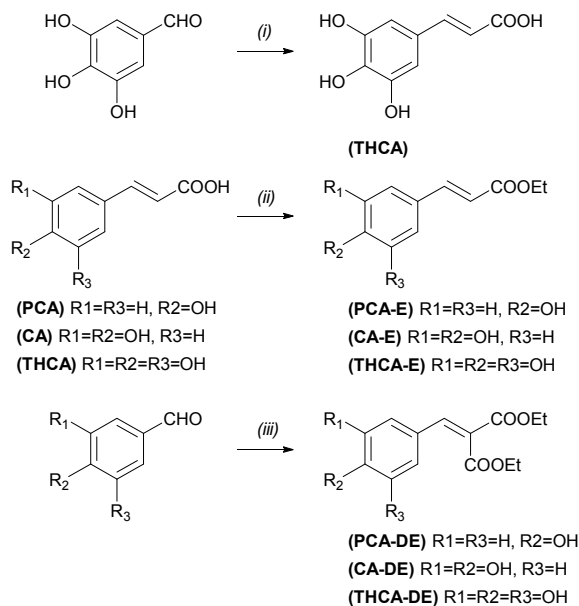
Scheme 1. Synthetic strategy followed to obtain free acid, ethyl ester and diethyl ester cinnamic derivatives. (i) Malonic acid, pyridine, piperidine, 50 ºC, 20 h; (ii) EtOH, H2SO4, 100 ºC, 20 h; (iii) diethyl malonate, pyridine, piperidine, 50 ºC, 20 h.

2.2 In vitro cyclooxygenase (COX) inhibition assay

The HCAs and their ester derivatives were evaluated for their inhibitory activity against COX-1 and COX-2 in human whole blood assay using in vitro measurement of the production of thromboxane B2 (TXB2) and prostaglandin E2 (PGE2), respectively. The derivatives were classified into three series (Scheme 1):

(A) Simple HCAs: p-coumaric acid (PCA), caffeic acid (CA) and 3,4,5-trihydroxy cinnamic acid (THCA);
(B) Ethyl esters of HCAs: PCA-E, CA-E and THCA-E;
(C) Diethyl esters of HCAs: PCA-DE, CA-DE and THCA-DE.

Thus, mono and diethyl ester derivatives of HCAs were synthesized and screened for COX-1/COX-2 inhibitory potential. Inhibition percentages of TXB2 and PGE2 formation were assessed at 100 and 20 µM of test compounds using a commercially available EIA kit (Enzo life sciences, Farmingdale, NY). The selectivity ratio (SR values) was defined as the ratio of the percentage of COX-2 inhibition to the percentage of COX-1 inhibition at the concentration of 100 µM for the compounds under study. Indomethacin at concentration of 500 nM was used as a non-selective reference inhibitor (SR = 0.97). The results of COX-1 and COX-2 inhibitory assays are summarized in Table 1. Simple HCAs (PCA, CA and THCA) were completely inactive or had a very low activity against both COX-1 and COX-2 isoforms. All 3 ethyl esters (PCA-E, CA-E and THCA-E) appeared to have higher COX-1 inhibitory activities compared to non-esterified parent HCAs. On the other hand, diethyl esters (PCA-DE, CA-DE and THCA-DE) seemed to have enhanced inhibitory activities towards COX-2 compared to their parental HCAs (Table 1). CA-DE was found to be the most selective COX-2 inhibitor with an SR of 9.1. This compound was also one of the most potent agents against COX-2 with an inhibition percentage of 88.5% at 100 µM. The second most selective inhibitor was PCA-DE with an SR of 5.8. PCA-DE was also one of the most potent COX-2 inhibitors and could inhibit the enzyme by 86.9% at 100 µM. THCA-DE also demonstrated high COX-2 inhibitory potential (84.4% inhibition at 100 µM), but with a lower selectivity (SR = 2.0). In view of the above mentioned results, the following structure-activity relationships (SAR) could be established for HCA derivatives:

-   Esterification of the carboxylic acid moiety of olefin side chain increases COX inhibitory activity;
-   Diethyl ester derivatives of different HCAs display a higher COX-2 inhibitory activity;
-   The manipulation of the number of phenolic OH groups combined with the esterification of the carboxylic side chain confers improvement in inhibitory potency and also selectivity towards COX-2.

COX-2 selective inhibitors have been given particular attention, because of their improved gastrointestinal safety profile.[10] On the other hand, COX-2 isoform, aside from its involvement in inflammatory processes, seems to be also involved in ageing diseases, such as Alzheimer disease and other neurodegenerative disorders and cancer.[8,37] Therefore compounds aimed at this target are desirable; however, serious concern has been raised regarding the cardiovascular adverse effects of previously launched tricyclic templates.[38]

RSC Advances

ARTICLE

Table 1. COX-1 and COX-2 enzyme inhibitory activities of hydroxycinnamic acid derivatives.

Compounds	% Inhibition COX-1[a,b]		% Inhibition COX-2[a,b]		SR[c]
	100 μM	20 μM	100 μM	20 μM	
PCA	NA[d]	NA[d]	NA[d]	NA[d]	---
PCA-E	67.5 ± 14.0	45.9 ± 9.4	NA[d]	NA[d]	---
PCA-DE	15.2 ± 2.3	5.2 ± 1.0	86.9 ± 2.5	13.1 ± 3.1	5.8
CA	NA[d]	NA[d]	15.5 ± 2.1	6.7 ± 1.0	---
CA-E	72.8 ± 11.6	52.0 ± 1.7	84.8 ± 4.2	19.1 ± 1.5	1.2
CA-DE	9.3 ± 0.3	9.7 ± 9.7	88.5 ± 4.9	30.5 ± 4.1	9.1
THCA	NA[d]	NA[d]	NA[d]	16.0 ± 9.3	---
THCA-E	73.3 ± 0.5	5.4 ± 3.4	10.8 ± 7.9	13.2 ± 1.2	0.15
THCA-DE	43.5 ± 2.4	19 ± 3.4	84.4 ± 9.0	36.1 ± 14.2	2.0
Indomethacin 500 nM	76.6 ± 5.2[e]		74.1 ± 14.0[e]		0.97

[a] Percentage of inhibition compared to control. [b] Values represent the mean ± S.E.M. of 3-4 different experiments. [c] Selectivity ratio at 100 μM (% COX-2 inhibition/% COX-1 inhibition) [d] Not active. [e] Percentage of inhibition was evaluated at 500 nM.

Abbreviations: p-Coumaric acid (PCA); p-coumaric acid ethyl ester (PCA-E); p-coumaric acid diethyl ester (PCA-DE); caffeic acid (CA); caffeic acid ethyl ester (CA-E); caffeic acid diethyl ester (CA-DE); trihydroxy cinnamic acid (THCA); trihydroxy cinnamic acid ethyl ester (THCA-E); trihydroxy cinnamic acid diethyl ester (THCA-DE).

Market withdrawal of some coxibs such as rofecoxib andvaldecoxib because of adverse thrombotic cardiovascular events were attributed either to an intrinsic chemical property related to their metabolism or to the biochemical imbalance in PGI2/TXA2 production associated with highly selective COX-2 inhibitors.[12,39]Therefore, the need for the development of other COX-2 inhibitor agents with improved safety profile seems to be compelling. This could probably be achieved by a more careful selection of compounds that have a moderate selectivity towards COX-2, since failed coxibs have generally had very high SR towards this isoform.[40]

2.3 Molecular docking studies

In order to achieve a better understanding of the COX inhibitory activity of designed HCA derivatives, which could serve consequent SAR studies, molecular docking studies of one of the potent COX-2 inhibitors of this series (CA-DE) were performed. The crystal structures of COX-1 (PDB code: 1EQG) and COX-2 [PDB code: 1CX2] enzymes complexed with known inhibitors were used for the molecular modeling studies. The active site of each enzyme was defined based on the center and the radius of any cognate inhibitor atom. The automated docking program of Autodock 4.2 [41] was used for the molecular docking study. The most stable docking model was selected according to the best scored conformation predicted by the Autodock 4.2 scoring function. Docking validation was performed based on the RMSD (root mean square deviation) of the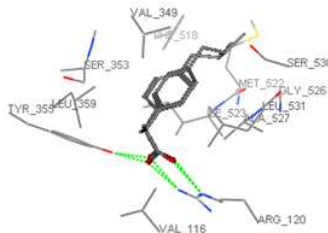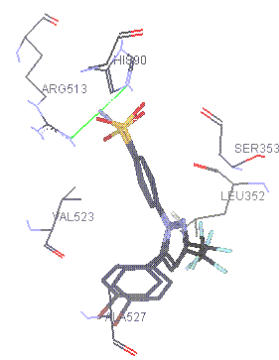 best-docked conformation of cognate ligand from experimental one (internal validation).[42]Accordingly, docking performance was examined by re-docking of the co-crystallized conformation of the native ligands into the corresponding enzyme's active site.The top-docking score pose of cognate ligand (ibuprofen and SC-558) was superimposed over the X-ray coordinates of experimentally derived structure bound to COX-1 and COX-2, respectively. The best-docked and actual conformation of ibuprofen correlated quite well with an RMSD of 0.943 Å and binding free energies of -8.58 kcal/mol. The RMSD and binding free energy values obtained as a result of the re-docking procedure of SC-558 into the COX-2 active site were 1.373 Å and -11.62 kcal/mol, respectively. It should be mentioned that the RMSD of lower than 2 Å is the commonly acceptable limit.[43]The results of the docking validation are presented in Table 2. A molecular docking study of CA-DE was performed according to the described validated procedure. The complex generated by docking studies of CA-DE with each COX isoform and superimposition with corresponding cognate ligand (derived from co-crystallization with the enzyme), indicated that the best scored conformation of CA-DE have fitted into the known classic binding cleft of COX-2 in similar manner as the pyrazolic COX-2 inhibitor, SC-558 (Fig. 3). In fact, the 3,4-dihydroxyphenyl moiety of CA-DE was positioned in the same region occupied by p-sulfonamidophenyl ring of SC-558.In addition, diethyl ester moieties of CA-DE were directed towards the aromatic region of the active site, which roughly mimics the p-Br-phenyl ring of SC-558 (Fig. 3B).

RSC Advances

ARTICLE

Table 2. Docking validation results for PDB structures of COX-1 (1EQG) and COX-2 (1CX2) using AutoDock4.2

PDB code	Binding mode of cognate inhibitor Within the active site*	No. GA run	Population in the optimum cluster (%)	RMSD from reference structure(Å)	Estimated free energy of binding (Kcal/Mol)
1EQG		100	100	0.943	-8.58
1CX2		100	96	1.373	-11.62

*Superimposed structure of the best docked poses of the cognate on the native ligands (ibuprofen and SC-558 for COX-1 and COX-2, respectively).
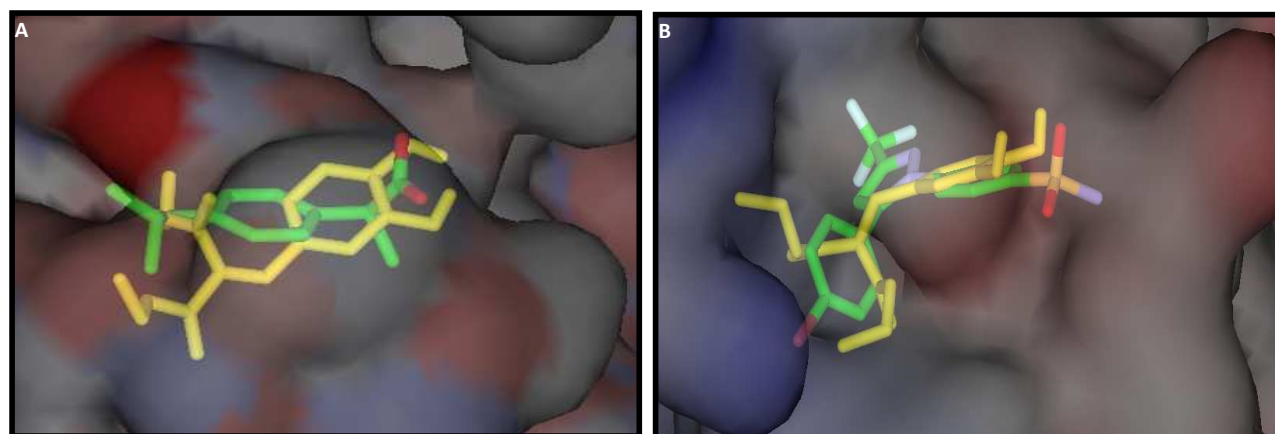

Figure 3. Comparative binding of caffeic acid diethyl ester (CA-DE) into the active sites of COX enzymes. **A.** Binding orientation of CA-DE (yellow) into the active site of COX-1 (ibuprofen shown in green) **B.** Binding orientation of CA-DE (yellow) in the COX-2 active pocket (SC-558 shown in green). The binding sites are depicted with solid surface.

The comparative binding mode of CA-DE in COX-1 showed that 3,4-dihydroxyphenyl ring of this compound is positioned towards the COX-1 active site similar to the propionic side chain of ibuprofen. One of the ethyl ester substituents of CA-DE was positioned in the COX-1 active site in the similar fashion as isobutylphenyl substitute of ibuprofen, while the other ester substituent displayed mild deviation from the COX-1 binding site (Fig. 3A). Further details of the binding interactions of CA-DE with the amino acid residues of the active sites of COX-1 and COX-2 are illustrated in Fig. 4. This compound was found to dock into the active site of COX-1 with an interactionenergy of -6.13 Kcal/mol. According to the obtained results, two hydrogen bonds between 4-OH of 3,4-dihydroxyphenyl of CA-DE and hydroxyl of Tyr355 (Tyr355-OH) and NH side chain of Arg120 (Arg120-NH, bond distance 2.7 and 3.1 Å, respectively) of COX-1 active pocket were observed. Fig. 4 also demonstrates the binding interaction of CA-DE (ΔG_b = -7.60Kcal/mol) within COX-2 binding pocket and the formation of three hydrogen bond interactions with the binding cleft of COX-2 as follows: two hydrogen bonds between 4-OH of CA-DE and Tyr355-OH (OH..OH) and Arg120-NH (OH..NH) (with bond distances of 2.7 and 3.3 Å, respectively) and a third hydrogen bond between C=O of ethyl ester substituent of CA-DE and Tyr385-OH (bond distance 3.0 Å). The greater interaction energy of CA-DE into the COX-2 active site, which might be attributed to its third hydrogen bonding with Tyr385, supports the tighter binding of CA-DE into COX-2 binding pocket. According to the previous studies, Tyr385 is involved in the abstraction of 13-pro-S-hydrogen from arachidonic acid.[44] The observed hydrogen bonding interaction between CA-DE and Tyr385, absent in the case of CA-DE/COX-1 complex, might be an explanation for the observed selectivity of CA-DE towards COX-2 inhibition. Furthermore, X-ray crystallographic analyses of COX-1 and COX-2 active pockets have demonstrated the existence of some differences between these two isoforms and have provided useful guidelines towards the design of selective COX-2 inhibitors. For instance, COX-2 has larger active site volume (-417 Å) when compared to COX-1 (-366 Å).[20,45]This difference has been attributed to the smaller size of valine side chain (Val523) in COX-2 binding site coupled with the conformational changes at Tyr355 that opens up the new hydrophobic pocket surrounded by Leu352, Ser353, Tyr355, Tyr348, Val523 and Phe518. This hydrophobic cleft also exists in COX-1 active site, but is inaccessible as a result of presence of larger and bulkier isoleucine residue, Ile523 instead of Val523.[45] As shown in Fig. 4, the two ethyl ester moieties of CA-DE were well accommodated into the available and exclusive hydrophobic pocket of COX-2 comprising of Phe518, Val523, Met522, Tyr385, Ser523 and provided favorable hydrogen bond interaction with Tyr385 of COX-2 active site. On the other hand, the presence of Ile523 at the entrance of hydrophobic cleft of COX-1 binding site introduces some steric clashes that hindered the accessibility of ethyl ester substituents to this hydrophobic site. The differences found between the binding interaction of CA-DE with COX-1 and

COX-2 can explain the selectivity found for the diethyl ester derivatives of HCAs towards COX-2 inhibition.
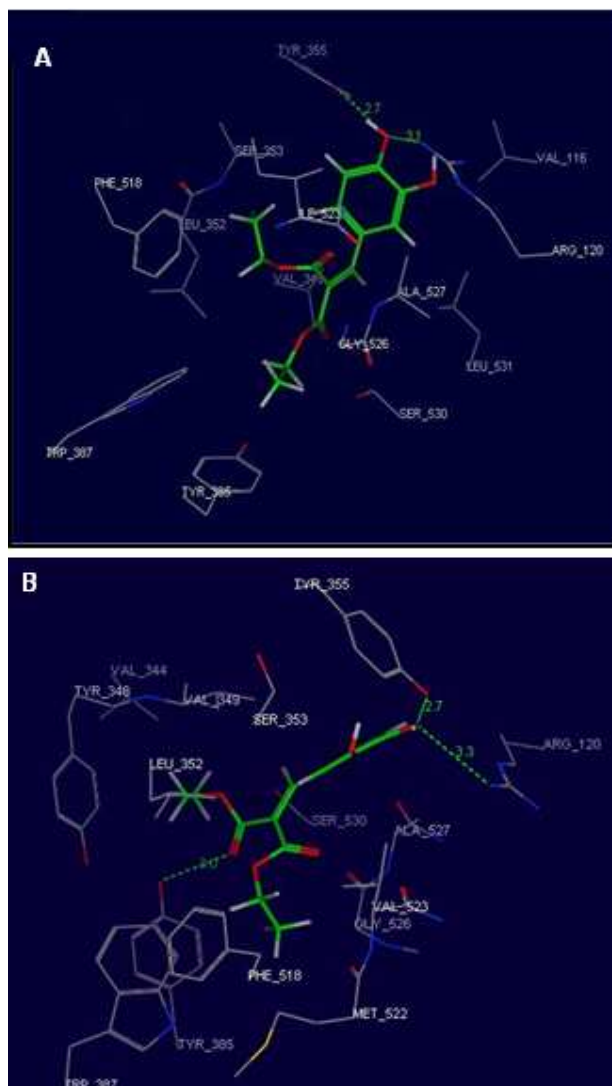

Figure 4. Best docking poses of caffeic acid diethyl ester (CA-DE) into the COX-1 (**5A**) and COX-2 (**5B**) binding sites. The ligand is depicted in stick model and the interacting residues are displayed in line style. Broken lines indicate hydrogen bond interactions.

In an attempt to evaluate the contribution of each amino acid-ligand interaction energy and further comparison of the interaction of CA-DE with COX-1 and COX-2, we employed *ab initio* method to calculate ligand-residue binding energy (ΔE_b) using our previously reported equation.[46] Binding energies of CA-DE with individual amino acid residues surrounding the COX-1 and COX-2 binding sites at the B3LYP/Def2-SVP level of calculation are summarized in Fig. 5A and 5B, respectively. CA-DE is involved in three hydrogen binding interactions with Arg120, Tyr355 and Tyr385 with respective estimated binding energies of -7.33, -18.86 and -15.44 kcal/mol in the COX-2 active site. The corresponding hydrogen binding energies of CA-DE with Arg120 and Tyr355 of COX1 catalytic site were -15.40 and -11.10 Kcal/mol, respectively. Comparison of

CA-DE-residue binding energy of COX-1 (6A) and COX-2 (6B) indicated a week interaction of CA-DE with Tyr385 of COX-1 catalytic site. Furthermore, the calculated total binding energy of CA-DE with catalytic residues of COX1 and COX2 enzymes ($E_{b\ (total)}$) were -179.67 and -209.79 kcal/mol, respectively. These differences could be attributed to other important ligand-residue interactions, such as hydrophobic and electrostatic interactions, resulting in increased inhibition of COX-2 by CA-DE.
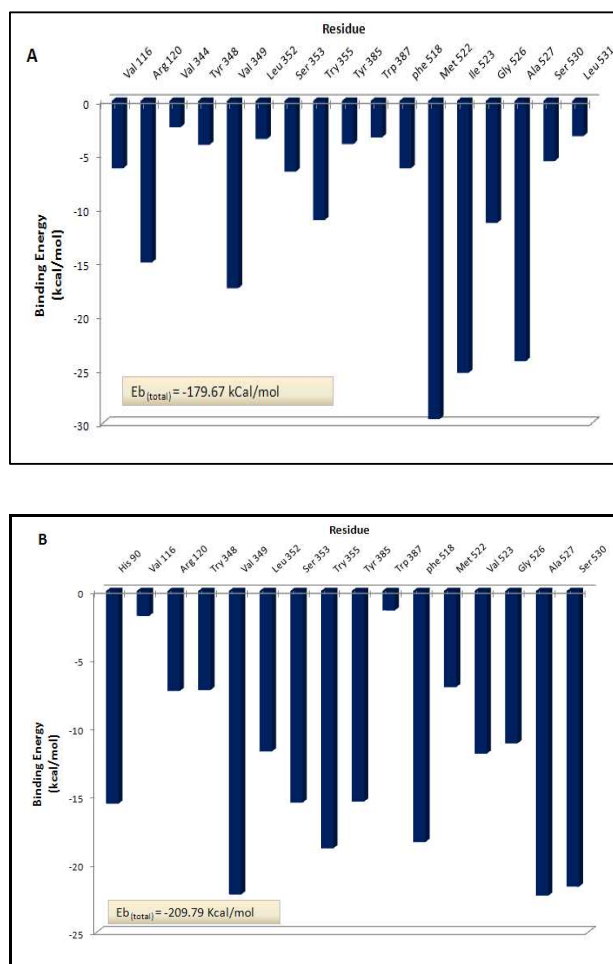

Figure 5. Binding energies of the interactions of CA-DE with the active site amino acid residues of COX-1 (**6A**) and COX-2 (**6B**).

3 Experimental

3.1 Chemistry

3.1.1. Reagents and materials

Caffeic acid (CA), p-coumaric acid (PCA), malonic acid and diethylmalonate were purchased from Sigma-Aldrich (Sintra, Portugal). All other reagents and solvents were pro analysis grade and were acquired from Merck (Darmstadt, Germany) and used without additional purification. Thin layer chromatography (TLC) analyses were performed on aluminium silica gel sheets 60 F254 plates from Merck and spots were detected using a UV lamp at 254 nm. Column chromatography purifications were performed with silica gel 60A (Carlo ErbaReactifs–SDS, France).

3.1.2 Apparatus

1H and 13C NMR data were acquired, at room temperature, on a Brüker AMX 300 spectrometer operating at 300.13 and 75.47 MHz, respectively. DMSO-d6 was used as solvent; chemical shifts are expressed in δ (ppm) values relative to tetramethylsilane (TMS) as internal reference; coupling constants (*J*) are given in Hz. Assignments were also made from DEPT (distortionless enhancement by polarization transfer) (underlined values). Electron impact mass spectra (EI-MS) were carried out on a VG AutoSpec instrument; the data are reported as *m/z* (% of relative intensity of the most important fragments). Microwave-assisted synthesis was executed in a Biotage® Initiator Microwave Synthesizer.

3.1.3 General synthetic procedures

General synthetic for microwave-assisted esterification
PCA-E, CA-E and THCA-E were synthesised by Fisher esterification according the general procedure previously described by our research group (Scheme 1).[34] Briefly, the acid (5 mmol) with the appropriate aromatic pattern, ethanol (2.5 mL) and H_2SO_4 (3 drops) were put together in a glass vial (2-5 mL) sealed with a cap and heated in the microwave reactor cavity under mechanical stirring at $100^{\circ}C$ for 20 minutes. After cooling to room temperature, the solvent was removed in vacuo, the residue was dissolved in ethyl acetate, (25 mL) and washed with $NaHCO_3$ and water (3 x 10 mL). The organic layer was dried over Na_2SO_4, filtered and concentrated under reduced pressure. The compounds were purified by flash chromatography (silica gel; CH_2Cl_2 with increasing methanol until 9.5:0.5) and recrystallized from diethyl ether/petroleum ether.

(E)-ethyl-3-(4-hydroxyphenyl)-2-propenoate (PCA-E)
Yield 65%; ^1H NMR δ(ppm): 1.25 (t, *J* = 7.10 Hz, 3H, OCH_2CH_3), 4.26 (q, *J* = 7.10 Hz, 2H, OCH_2CH_3), 6.48 (d, *J* = 16.0 Hz, H(α)), 6.79 (m, 2H, H3, H5), 7.56 (m, 3H, H2, H6, Hβ), 9.99 (s, 1H, C4-OH); ^{13}C NMR δ(ppm): 14.7 (OCH_2CH_3), 61.2 (OCH_2CH_3), 114.8 (Cα), 116.2 (C3,C5), 125.6 (C1), 130.7 (C2,C6), 145.0 (Cβ), 160.3 (C4), 167.1 (C=O); EI-MS m/z (%): 192 (M+., 80), 164 (19), 148 (100), 120 (35), 89 (27); mp [65-67]^{o}C.

(E)-ethyl-3-(3,4-dihydroxyphenyl)-2-propenoate (CA-E)
Yield 65%; ^1H NMR δ(ppm): 1.24 (t, *J* = 7.10 Hz, 3H, OCH_2CH_3), 4.15 (q, *J* = 7.09 Hz, 2H, OCH_2CH_3), 6.25 (d, *J* = 15.9 Hz, 1H, H(α)), 6.75 (d, *J* = 8.12 Hz, 1H, H5), 7.00 (dd, *J* = 8.28, 2.07 Hz, 1H, H6), 7.04 (d, *J* = 2.08 Hz, 1H, H2), 7.46 (d, *J* = 15.9 Hz, 1H, Hβ), 9.12 (s, 1H, OH), 9.57 (s, 1H, OH); ^{13}C NMR δ(ppm): 13.7 (OCH_2CH_3), 59.1 (OCH_2CH_3), 113.5 (C2), 114.2 (C5), 120.7 (C6), 118.2 (Cα), 124.9 (C1), 144.4 (Cβ), 145.0 (C-OH), 147.8 (C-OH), 165.9 (C=O); EI-MS *m/z* (%): 208 (M$^{+\cdot}$, 81), 199 (21), 180 (17), 163 (100), 145 (13), 136 (31), 89 (23); mp [140-145]^{o}C.

(E)-ethyl-3-(3,4,5-trihydroxyphenyl)-2-propenoate (THCA-E)

Yield 65%; ^{1}H NMR δ(ppm): 1.36 (t, J = 7.13 Hz, 3H, OCH$_2$CH$_3$), 4.29 (q, J = 7.12 Hz, 2H, OCH$_2$CH$_3$), 6.37 (d, J = 15.9 Hz, 1H, Hα), 6.78 (s, 2H, H2, H6), 7.62 (d, J = 15.9 Hz, 1H, Hβ), 8.80 (s, 1H, C4-OH), 9.18 (s, 2H, C3-OH, C5-OH); ^{13}C NMR δ(ppm): 15.2 (OCH$_2$CH$_3$), 61.4 (OCH$_2$CH$_3$), 106.2 (C2,C6), 118.2 (Cα), 130.9 (C1), 141.0 (C4), 145.5 (Cβ), 154.3 (C3,C5), 167.9 (C=O); EI-MS m/z (%): 224 (M$^{+\cdot}$, 100), 196 (17); 179 (86), 152(48), 133 (40), 105 (21), 77 (32); mp [176–179]^{o}C.

General synthetic procedure for Knoevenagel-Doebner condensation

THCA, PCA-DE, CA-DE and THCA-DE were synthesized following a variation of a process previously described (Scheme 1).[34] Accordingly, the Knoevenagel-Doebner condensation was performed between the corresponding hydroxybenzaldehyde (1 g) and malonic acid (1 g) (for THCA) or diethylmalonate (1.6 mL) (for PCA-DE, CA-DE and THCA-DE), in pyridine (5 mL) using piperidine (four drops) as catalyst. The reactions took place under reflux at 50 ºC for 20 h. The mixtures were diluted with ethyl acetate (10 mL) and washed with HCl 1 M and water (3 x 10 mL). The organic layers were then dried over Na$_2$SO$_4$, filtered and concentrated under reduced pressure. The compounds were purified by flash chromatography (silica gel; ethyl acetate/n-hexane (7:3) for CA-DE and THCA-DE and dichloromethane/methanol (9:1) for THCA and PCA-DE).

Diethyl 2-(4-hydroxybenzylidene)malonate (PCA-DE)

Yield 25%; ^{1}H NMR (400 MHz) δ(ppm): 1.25 (t, J = 7.10 Hz, 6H, 2x OCH$_2$CH$_3$), 4.22 (q, J = 7.09 Hz, 2H, OCH$_2$CH$_3$), 4.30 (q, J = 7.11 Hz, 2H, OCH$_2$CH$_3$), 6.84 (m, 2H, H3, H5), 7.38 (m, 2H, H2, H6), 7.59 (s, 1H, Hβ), 10.27 (s, 1H, OH); ^{13}C NMR (100 MHz) δ(ppm): 15.1 (OCH$_2$CH$_3$), 15.4 (OCH$_2$CH$_3$), 62.4 (OCH$_2$CH$_3$), 62.6 (OCH$_2$CH$_3$), 117.3 (C3,C5), 123.2 (C1), 124.4 (Cα), 133.3 (C2,C6), 142.7 (Cβ), 161.7 (C4), 165.2 (C=O), 167.9 (C=O); EI-MS m/z (%): 264 (M$^{+\cdot}$, 100), 219 (85), 190 (34), 146 (35), 118 (81), 91 (15), 63 (19); mp[89-93]^{o}C.

Diethyl 2-(3,4-dihydroxybenzylidene)malonate (CA-DE)

Yield 52%; ^{1}H NMR δ(ppm): 1.24 (m, 6H, 2xOCH$_2$CH$_3$), 4.20 (q, J = 7.10 Hz, 2H, O CH$_2$CH$_3$), 4.30 (q, J = 7.10 Hz, 2H, OCH$_2$CH$_3$), 6.76 (d, J = 8.10 Hz, 1H, H5), 6.87 (dd, J = 8.39, 2.19 Hz, 1H, H6), 6.90 (d, J = 2.14 Hz, 1H, H2), 7.47 (s, 1H, Hβ); ^{13}C NMR δ(ppm): 14.2 (OCH$_2$CH$_3$), 14.5 (OCH$_2$CH$_3$), 61.4 (OCH$_2$CH$_3$), 61.7 (OCH$_2$CH$_3$), 110.4, 116.1 (C2,C5), 122.0 (C1), 123.9 (Cα), 124.3 (C6), 142.1 (Cβ), 146.0 (C-OH), 149.7 (C-OH), 164.4 (C=O), 167.0 (C=O); EI-MS m/z (%): 280 (M$^{+\cdot}$, 100), 235 (34), 206 (38), 189 (39), 161 (41), 134 (92), 105 (24), 77 (25); mp [131-135]^{o}C.

(E)-3-(3,4,5-trihydroxyphenyl)-2-propenoic acid (THCA)

Yield 35%; ^{1}H NMR δ(ppm): 6.09 (d, J = 15.8 Hz, 1H, Hα), 6.57 (s, 2H, H2, H6), 7.32 (d, J = 15.8 Hz, 1H, Hβ), 8.74 (s, 1H, C4-OH), 9.17 (s, 2H, C3-OH, C5-OH); ^{13}CNMR δ(ppm): 107.5(C2,C6), 115.2 (Cα), 124.6 (C1), 136.3 (C4), 145.1 (Cβ), 146.2 (C3,C5), 168.0 (C=O); EI-MS m/z (%): 196(M$^{+\cdot}$, 100), 179

(22); 152 (57), 133 (27), 105 (16), 78 (51),63 (57); mp [186–188]^{o}C.

Diethyl 2-(3,4,5-trihydroxybenzylidene)malonate (THCA-DE)

Yield 70%; ^{1}H NMR δ(ppm): 1.33 (t, J = 7.13 Hz, 6H, 2xOCH$_2$CH$_3$), 4.28 (q, J = 7.13 Hz, 2H, OCH$_2$CH$_3$), 4.36 (q, J = 7.14 Hz, 2H, OCH$_2$CH$_3$), 6.57 (s, 2H, H2, H6), 7.52 (s, 1H, Hβ), 8.21 (s, 1H, C4-OH), 8.81 (s, 2H, C3-OH, C5-OH); ^{13}C NMR δ(ppm): 14.4 (OCH$_2$CH$_3$), 14.8 (OCH$_2$CH$_3$), 62.4 (OCH$_2$CH$_3$), 62.7 (OCH$_2$CH$_3$), 110.4 (C2,C6), 123.3 (C1), 124.6 (Cα), 137.2 (C4), 144.1 (Cβ), 146.1 (C3,C5), 165.7 (C=O), 168.8 (C=O); EI-MS m/z (%): 296 (M+., 100), 251 (36), 222 (38), 205 (49), 178 (38), 150 (58); mp [182–184]^{o}C.

3.2 *in vitro* screening for COX inhibition

3.2.1. Inhibition of COX-1 activity in human whole blood

COX-1 activity was determined by measuring the production of thromboxane B2 (TXB2), produced during the spontaneous clotting of human whole blood. Fresh human venous blood from three healthy donors was collected in glass tubes without anticoagulant, one volunteer each day. The volunteers had not taken any non-steroidal antiinflammatory drugs (NSAIDs) for two weeks prior to sampling. Aliquots of blood (0.5 mL) were immediately transferred to tubes containing 2 μL of inhibitor or vehicle (DMSO). Samples were vortex-mixed and incubated at 37 ºC for 1 h. Then, the tubes were centrifuged at 5000 × g for 10 min and 60 μL of serum was mixed with 240 μL of methanol in order to precipitate the proteins. Samples were centrifuged again and the supernatants were taken for measurements of TXB2 by a commercially available EIA kit (Enzo life sciences, Farmingdale, NY). Samples were tested at two different concentrations (100 and 20 μM) and percentages of inhibition of TXB2 production were calculated at each examined concentration as compared to the control.

3.2.2. Inhibition of COX-2 activity in human whole blood

COX-2 activity was determined by measuring the formation of prostaglandin E2 (PGE2), after incubation of blood samples with lipopolysaccharide (LPS from Escherichia coli serotype 0111-B4; Sigmaaldrich) according to a previously described method.[30,47] Fresh venous blood from healthy volunteers was collected in tubes containing heparin (15 IU/mL). None of the volunteers had taken any NSAIDs for two weeks prior to sampling. Half mL of blood was transferred to tubes containing 2 μL of inhibitor or DMSO and incubated at 37°C for 15 min. Then, 6 μL of LPS solution (final concentration 30 μg/mL) was added to each tube and the samples were further incubated at 37°C for 18 h. After the separation of plasma, proteins were precipitated as described above and levels of PGE2 were measured by a commercially available EIA kit (Enzo life sciences, Farmingdale, NY). Test samples were examined at two different concentrations (100 and 20 μM) and percentages of inhibition of PGE2 production were calculated at each tested concentration as compared to the control.

3.3. Molecular modeling methods

3.3.1. Molecular docking study

Autodock 4.2 and Auto Dock Tools 1.5.4 (ADT) were used for the docking study. The X-ray crystal structure of both COX-1/ibuprofen (a non-selective inhibitor) and COX-2/SC-558 (a selective inhibitor) complexes (PDB codes: 1EQG and 1CX2, respectively) were retrieved from the Protein Data Bank (http://www.rcsb.org) and used as templates to construct the three-dimensional models for all the compounds under study. Water molecules and cognate ligands were removed from the receptor. All hydrogens were properly added to the receptor PDB and non-polar hydrogens were merged into related carbon atoms of the receptor using ADT. Kollman charges were also assigned.The three-dimensional structure of CA-DE was constructed using Chem3D Ultra 8.0 and energetically minimized (100 steepest descent steps using MM + force field with a gradient convergence value of 0.1 kcal/mol) using HyperChem software. The Gastiger charges (empirical atomic partial charges) and torsional degrees of freedom were assigned on the generated PDB files by ADT 1.5.4. The grid maps of COX-1 and COX-2 were calculated with AutoGrid (part of the AutoDock package). The created three-dimensional grids were $60 \times 60 \times 60$ (x, y, z) with a grid spacing of 0.375 Å and the cubic grids were centered on the binding site of native ligand of each receptor.Automated docking studies were carried out using Lamarckian Genetic Algorithm (LGA). For LGA method; 2,500,000 energy evaluation, population size of 150, a gene mutation rate of 0.02; a crossover rate of 0.8 and number of 100 independent docking runs were used for each case. Cluster analysis was performed on the docked results using a root mean square (RMS) tolerance of 2.0 Å. After validating of our computational modeling approach in which X-ray structures served as reference structures for the calculation of the root mean square deviation (RMSD), the same modelling computational protocols were applied to the target compounds.

3.3.2. Amino acid decomposition analysis

In order to calculate the binding energies of docked ligand with each active site amino acid residue of COX-1 and COX-2 enzymes, the B3LYP/Def2-SVP method was employed. The evaluated amino acid residues were chosen based on the ligand-receptor interaction profile obtained from docking results. All amino acids were considered in their real electronic state. For each residue under study, N-terminal was acetylated and C-terminal was methyl amidated to mimic the original electron density. All the interaction energies were estimated by functional B3LYP associated with split valence basis set using polarization functions (Def2-SVP). The whole calculations were done using an ORCA quantum chemistry package.[48] Ligand-residue binding energies (ΔE_b) were calculated using our previously introduced equation.[46]

4 Conclusions

In this study, we have reported the COX inhibitory activity of HCAs (PCA, CA and THCA) and their ethyl and diethyl esters. Ethyl ester derivatives (PCA-E, CA-E and THCA-E), display COX-1inhibitory activity, while diethyl esters (PCA-DE, CA-DE and THCA-DE), particularly CA-DE, had COX-2 selectivity. The selective COX-2 inhibition by CA-DE can be attributed to the formation of 3 hydrogen bonds with the active site of COX-2 (4-OH..OH-Tyr355, 4-OH..NH-Arg120 and C=O..OH-Tyr385) vs 2 hydrogen bonds formed with COX-1 (4-OH..OH-Tyr355 and 4-OH..NH-Arg120), as shown by the docking studies performed with this compound on both enzyme isoforms. Thus, it can be concluded that with simple chemical modifications of a natural scaffold present in human diet, selective inhibition of COX-2 was achieved. Furthermore, the obtained results encourage the progress of the current drug discovery program with the development of additional sets of HCA derivatives bearing bioisosteric modifications, such as amides and other electronically equivalent groups. The gathered data strengthens the importance of exploring cinnamic scaffold as a template to build new chemical entities for inflammatory-associated diseases as well as pathologies such neurodegenerative diseases and cancer in which COX-2 seems to play an important role.

Acknowledgements

References

1　G. Dannhardt and W. Kiefer,*Eur J Med Chem*, 2001. **36**, 109-126;

2　W.L. Smith and R. Langenbach, *J Clin Invest*, 2001. **107**, 1491-1495.

3　P.C. Konturek, J. Kania, G. Burnat, E.G. Hahn andS.J. Konturek SJ.*J PhysiolPharmacol*, 2005. **56**, 57-73.

4　E. Ricciotti and G.A. FitzGerald, *ArteriosclerThrombVascBiol*, 2011. **31**, 986-1000.

5　Z. Khan, N. Khan, R.P. Tiwari, N.K. Sah, G.B. Prasad and P.S. Bisen, *Curr Drug Targets*.2011, **12**, 1082-1093.

6　P. Patrignani, S. Tacconelli, M.G. Sciulli, M.L. Capone, *Brain Res Brain Res Rev*. 2005, **48**, 352-359.

7　M. Etminan, S. Gill and A. Samii A, *BMJ*. 2003, **327**, 128.

8　S. Kraus, I. Naumov and N. Arber, *Recent Results Cancer Res*. 2013,**191**, 95-103.

9　M.M. Wolfe, D.R. Lichtenstein and G. Singh, *N Engl J Med*. 1999,**340**, 1888-1899.

10　A. Rostom, K. Muir, C. Dubé, E. Jolicoeur, M. Boucher, J. Joyce, P. Tugwell, G.W. Wells.ClinGastroenterolHepatol. 2007, **5**, 818-828.

11 A.K. Chakraborti, S.K. Garg, R. Kumar, H.F. Motiwala andP.S. Jadhavar, *Curr Med Chem*. 2010, **17**, 1563-93.

12 J.A. Baron, R.S. Sandler, R.S. Bresalier, A. Lanas, D.G. Morton, R. Riddell, E.R. Iverson and D.L. Demets. Lancet, 2008. **372**, 1756-1764.

13 C.D. Funk and G.A. FitzGerald, *J CardiovascPharmacol*, 2007. **50**, 470-479.

14 A.S. Kalgutkar, A.B. Marnett, B.C. Crews, R.P. Remmel andL.J. Marnett, *J Med Chem*. 2000, **43**, 2860-2870.

15 G.H. Hegazy and H.I. Ali, *Bioorg Med Chem*, 2012. **20**, 1259-1270.

16 A.S. Kalgutkar, B.C. Crews, S. Saleh, D. Prudhomme andL.J. Marnett, *Bioorg Med Chem*, 2005. **13**, 6810-6822.

17 M. Biava, G.C. Porretta, G. Poce, S. Supino, S. Forli, M. Rovini, A. Cappelli, F. Manetti, M. Botta, L. Sautebin, A. Rossi, C. Pergola, C. Ghelardini, E. Vivoli, F. Makovec, P. Anzellotti, P. Patrignani and M. Anzini, *J Med Chem*. 2007, **50**, 5403-5411.

18 A.S. Kalgutkar, B.C. Crews, S.W. Rowlinson, A.B. Marnett, K.R. Kozak, R.P. Remmel and L.J.Marnett, *ProcNatlAcadSci USA*. 2000, **97**, 925-930.

19 J.L. Mao, X.K. Ran, J.Z. Tian, B. Jiao, H.L. Zhou, L. Chen andZ.G. Wang, *Bioorg Med ChemLett*. 2011, **21**, 1549-1553.

20 R. Gautam, S.M. Jachak, V. Kumar and C.G. Mohan, *Bioorg Med ChemLett*, 2011. **21**, 1612-1616.

21 N. Razzaghi-Asl, J. Garrido, H. Khazraei, F. Borges and O. Firuzi, *Curr Med Chem*. 2013, **20**, 4436-4450.

22 J. Garrido, A. Gaspar, E.M. Garrido, R. Miri, M. Tavakkoli, S. Pourali , L. Saso, F. Borges and O. Firuzi, Biochimie, 2012. **94**, 961-967.

23 A. Gaspar, M. Martins, P. Silva, E.M. Garrido, J. Garrido, O. Firuzi, R. Miri, L. Saso and F. Borges, *J Agric Food Chem*. 2010, **58**, 11273-11280.

24 Y.M. Chiang, C.P. Lo, Y.P. Chen, S.Y. Wang, N.S. Yang, Y.H. Kuo and L.F. Shyur, *Br J Pharmacol*, 2005. **146**, 352-363.

25 A. Rossi, A. Ligresti, R. Longo, A. Russo, F. Borrelli and L. Sautebin, *Phytomedicine*. 2002, **9**, 530-535.

26 A. Rossi, R. Longo, A. Russo, F. Borrelli and L. Sautebin L, *Fitoterapia*. 2002, **73**, S30-S37.

27 M.H. Yang, K.D. Yoon, Y.W. Chin, J.H. Park and J. Kim, *Bioorg Med Chem.* 2009, **17**, 2689-2694.

28 N. Márquez, R. Sancho, A. Macho, M.A. Calzado, B.L. Fiebich, E. Muñoz, *J Pharmacol Exp Ther*. 2004, **308**, 993-1001.

29 H. Li, F. Zhu, Y. Sun, B. Li, N. Oi, H. Chen, R.A. Lubet, A.M. Bode and Z. Dong, *PLoS One*. 2013, **8**, e76452.

30 A. Moradi, L. Navidpour, M. Amini, H. Sadeghian, H. Shadnia, O. Firouzi, R. Miri, S.E. Ebrahimi, M. Abdollahi, M.H. Zahmatkesh andA. Shafiee, *Arch Pharm*. 2010, **343**, 509-518.

31 C. Siquet, F. Paiva-Martins, J.L. Lima, S. Reis and F. Borges, *Free Radic Res*. 2006, **40**, 433-442.

32 F.A. Silva, F. Borges, C. Guimarães, J.L. Lima, C. Matos and S. Reis, *J Agric Food Chem*. 2000, **48**, 2122-2126.

33 L. Navidpour, M. Amini, R. Miri, O. Firuzi, M. Tavakkoli and A. Shafiee, *J Heterocyclic Chem*. 2014, **51**, 71-79.

34 J. Teixeira, T. Silva, S. Benfeito, A. Gaspar, E.M. Garrido, J. Garrido and F. Borges F, *Eur J Med Chem*. 2013, **62**, 289-296.

35 M. Esteves, C. Siquet, A. Gaspar, V. Rio, J.B. Sousa, S. Reis, M.P. Marques and F. Borges,*Arch Pharm*. 2008, **341**, 164-173.

36 F.A. Silva, F. Borges, C. Guimarães, J.L. Lima, C. Matos and S. Reis, *J Agric Food Chem*. 2000, **48**, 2122-2126.

37 P. Teismann,Biofactors. 2012, **38**, 395-397.

38 O. Firuzi and D. Praticò, *Ann Neurol*. 2006, **59**, 219-228.

39 T. Grosser, Y. Yu and G.A. Fitzgerald, *Annu Rev Med*. 2010, **61**, 17-33.

40 S.D. Martina, K.S. Vesta and T.L. Ripley, *Ann Pharmacother*. 2005, **39**, 854-862.

41 G.M. Morris, R. Huey, W. Lindstrom, M.F. Sanner, R.K. Belew, D.S. Goodsell and A.J. Olson, *J Comput Chem*. 2009, **30**, 2785-91.

42 Y. Fukunishi, Y. Mikami and H. Nakamura, *J Mol Graph Model*. 2005, **24**, 34-45.

43 N. Edraki, O. Firuzi, A. Foroumadi, R. Miri, A. Madadkar-Sobhani, M. Khoshneviszadeh and A. Shafiee, *Bioorg Med Chem*. 2013, **21**, 2396-2412.

44 E.D. Thuresson, K.M. Lakkides, C.J. Rieke, Y. Sun, B.A. Wingerd, R. Micielli, A.M. Mulichak, M.G. Malkowski, R.M. Garavito and W.L. Smith, J Biol Chem. 2001, 276, 10347-10357.

45 A.L. Blobaum and L.J.Marnett, *J Med Chem*. 2007, **50**, 1425-1441.

46 N. Razzaghi-Asl , A. Ebadi, N. Edraki, S. Shahabipour and R, Miri*, Med Chem Res.* 2012, **22**, 3259-3269.

47 J.K. Gierse, Y. Zhang, W.F. Hood, M.C. Walker, J.S. Trigg, T.J. Maziasz, C.M. Koboldt, J.L. Muhammad, B.S. Zweifel, J.L. Masferrer, P.C. Isakson and K. Seibert, *J PharmacolExpTher*. 2005, **312**, 1206-1212.

48 F. Neese F. ORCA—an ab initio, density functional and semiempirical program package, version 2.8.0. University of Bonn, Bonn, 2011.